Med Chem Res (2013) 22:6154–6162
DOI 10.1007/s00044-013-0613-5

MEDICINAL CHEMISTRY RESEARCH

ORIGINAL RESEARCH

^{99m}Tc-labeled butyl-substituted zoledronic acid as a novel potential SPECT imaging agent: preparation and preclinical pharmacology study

Ling Qiu · Jianguo Lin · Wen Cheng · Yan Wang · Shineng Luo

Received: 20 February 2013 / Accepted: 2 May 2013 / Published online: 12 May 2013

Abstract Zoledronic acid (ZL) is the most potent among the tested diphosphonates. To develop a superior bone imaging agent that could improve the efficiency of bone scanning, an optimized radiotracer was designed from ZL and prepared successfully, ^{99m}Tc-BIDP [BIDP, 1-hydroxy-2-(2-butyl-1H-imidazole-1-yl) ethylidene-1,1-diphosphonic acid]. It possesses high radiolabeling yield, radiochemical purity, and stability. The biodistribution in mice shows that ^{99m}Tc-BIDP has high specificity in the skeleton with the maximum uptake of 24.6 ± 1.65 % ID g^{-1} at 120 min post injection. It can be quickly absorbed and rapidly eliminated from the blood judged from the short distribution half-life ($t_{1/2\alpha}$ = 1.65 min) and elimination half-life ($t_{1/2\beta}$ = 30.91 min). The bone imaging of the rabbit showed that ^{99m}Tc-BIDP has highly selective uptake in the skeletal system and rapid clearance from the soft tissues. An excellent scintigraphic image can be obtained at 1 h with clear visualization of the skeleton.

Keywords Zoledronic acid · ^{99m}Tc radiolabeling · Biodistribution · SPECT · Bone imaging

Introduction

Diphosphonates (DPs) are one of the important class of clinical drugs for bone disease (Vasireddy *et al*., 2003) and have been used in the therapy of early cancer treatment to prevent adverse effects of therapies on the bone health (Robert *et al*., 2011). They have experienced three generations. ZL is one typical third-generation DP and the most potent among the tested diphosphonates. For example, in preclinical models of bone resorption, ZL is at least 100 times more potent than either clodronate or pamidronate and it is at least 1,000 times more potent than etidronate (Smith, 2008).

As well known, DPs are good targeting ligands to serve as bone imaging agents (Jurisson *et al*., 1999). Up to date, a plenty of ^{99m}Tc-labeled DPs, such as ^{99m}Tc-MDP (Subramanian *et al*., 1975), ^{99m}Tc-HMDP (Bevan *et al*., 1980), and ^{99m}Tc-EHDP (Subramanian *et al*., 1972), have been widely used for many years in the clinical bone scanning. However, ^{99m}Tc-labeled DPs also present a set of clinical and chemical limitations (Vasireddy *et al*., 2003), such as the low specificity and relatively slow clearance from the blood and soft tissues, which usually leads to false negatives and delaying interval (2–6 h) between injecting and performing bone scanning (Love *et al*., 2003). To address these problems, a radiopharmaceutical with higher affinity for bone, lower tissue uptake, and more rapid clearance from the blood is required accordingly. Considering that the nature of ligand, DPs is a key factor in determining the performance of the bone imaging agent (Ogawa *et al*., 2006), so a novel diphosphonic acid was designed and synthesized to enable imaging at an earlier time.

To date, a number of ^{99m}Tc-labeled MDP analogs have been prepared and evaluated in animals (Pauwels *et al*., 2001; Love *et al*., 2003). We have also been involved for several years in the synthesis and biological evaluation of novel ^{99m}Tc-diphosphonate complexes for developing novel bone imaging agents (Luo *et al*., 2005; Niu *et al*., 2008; Chen *et al*., 2009; Lin *et al*., 2011). Previous studies have shown that optimization of the alkyl substituent in the imidazole ring of ZL or the carbon chain between the

L. Qiu · J. Lin (✉) · W. Cheng · Y. Wang · S. Luo
Key Laboratory of Nuclear Medicine of Ministry of Health, Jiangsu Key Laboratory of Molecular Nuclear Medicine, Jiangsu Institute of Nuclear Medicine, Wuxi 214063, China
e-mail: linjianguo@jsinm.org

imidazolyl and geminal diphosphonate groups can bring significant influence on the biological properties of ^{99m}Tc-labeled complexes, including the bone uptake, blood, and soft tissues clearance. In a continuing effort to look for better bone imaging agent, therefore, a novel ZL derivative was designed and synthesized, 1-hydroxy-2-(2-butyl-1H-imidazole-1-yl) ethylidene-1,1-diphosphonic acid (BIDP, see Scheme 1). It was further labeled by the radionuclide technetium-99m. The in vivo biological performances of ^{99m}Tc-BIDP, such as the biodistribution, pharmacokinetics, and bone imaging, were investigated systematically.

Materials and methods

Reagents, instruments, and animals

All analytical chemical reagents were purchased from commercial sources and used without further purification. Mouse serum (MS) (through the centrifugal homemade) and human serum (HS) (supplied by Jiangyuan Hospital of Jiangsu Institute of Nuclear Medicine) were used for in vitro stability study. Technetium-99m was eluted as $Na^{99m}TcO_4$ from $^{99}Mo/^{99m}Tc$ generator (radiochemical purity: 99.99 %; Jiangyuan Hospital of Jiangsu Institute of Nuclear Medicine).

Melting points were measured on Yanaco MP-500 melting point apparatus (Shimadzu, Japan). Electron spray ion mass spectra (ESI–MS) were determined using a Waters Platform ZMD4000 LC/MS (Waters, USA). ^{1}H and ^{13}C nuclear magnetic resonance (NMR) spectra were recorded on a Bruker DRX-500 spectrometer (Bruker, Germany), and the chemical shift values were referenced to the internal tetramethylsilane (TMS). The IR spectra were recorded on a Bruker TENSOR-27 spectrometer (Bruker, Germany) using KBr pellet in the region of 4,000–400 cm^{-1}. The Xinhua chromatography paper (Shanghai, China) was used for thin layer chromatography (TLC). Analytic high performance liquid chromatography (HPLC) were accomplished on Waters 1525 Binary HPLC pump, a Waters 2487 dual λ absorbance detector, and a Perkin Elmer Radiomatic 610TR radioactivity detector, which were operated by Breeze and proFSA software. A Packard-multi-prias γ Counter (Perkins Elmer, USA) were used for the radioactivity counting.

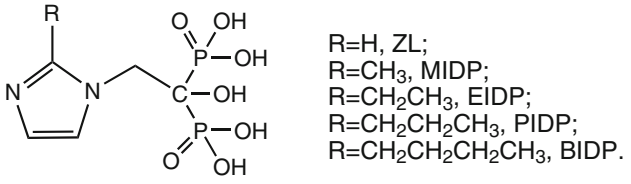

Scheme 1 Chemical structures of the DP ligands

Philips SKY Light emission computed tomography (ECT) (Philips, USA) was used for the bone scanning of the rabbit.

Institute of Cancer Research (ICR) mice (18–22 g) and New Zealand rabbit (1.5–1.7 kg) were supplied by Shanghai SLAC Laboratory Animal Company. Animals are bred according to the standards set forth in the Guide for the Care and Use of Laboratory Animals (published by the National Academy of Science, National Academy Press, Washington, DC). All procedures and animal protocols were approved by our Institutional Animal Experimentation Committee.

Synthesis and radiolabeling

BIDP was synthesized according to the similar method as reported in the previous literatures (Lin *et al.*, 2011; Widler *et al.*, 2002). The synthesis route has been summarized in Scheme 2. In brief, BIDP (5 mg, dissolved in 0.1 mL 0.2 M NaOH solution), $SnCl_2{\cdot}2H_2O$ solution (100 μL, freshly prepared, 10 mg $SnCl_2{\cdot}2H_2O$ dissolved in 10.0 mL 0.5 M HCl solution), and $Na^{99m}TcO_4$ (92.50 MBq freshly eluted) were added into a penicillin vial in turn. The pH of the mixture was adjusted to pH = 6.0 by adding 0.2 M phosphate buffer solution (PBS). The final volume of the solution was adjusted to 2.0 mL by water. The reaction mixture was heated at 70 °C for 30 min.

Quality control

The radiolabeling yield (RLY) and radiochemical purity (RCP) of ^{99m}Tc-BIDP were determined by TLC method. Strips of Xinhua No. 1 paper chromatography of 13 cm long and 0.5 cm wide were marked at 1.5 cm from the bottom and lined into sections 1 cm each, up to 10 cm. About 3 μL ^{99m}Tc-BIDP solution was applied with a syringe at 1.5 cm from the bottom of paper strips, and then the strips were developed in distilled water and acetone. After complete development, the chromatographic paper strips were cut into pieces of 1 cm and the radioactivity of these pieces was counted by a γ counter to determine the RLY and RCP.

At the same time, the RLY and RCP of ^{99m}Tc-BIDP were also measured by HPLC method. The column was eluted with isocratic solvents of 70 % water and 30 % acetonitrile, and the flow rate was 1.0 mL min^{-1}. Radioanalysis of the labeled compound was performed using a Cd (Te) detector.

In vitro stability

The in vitro stability of ^{99m}Tc-BIDP was studied in mouse serum (MS) and human serum (HS) for 1–6 h. In brief, 200 μL (about 3.7 MBq) of ^{99m}Tc-BIDP was added into

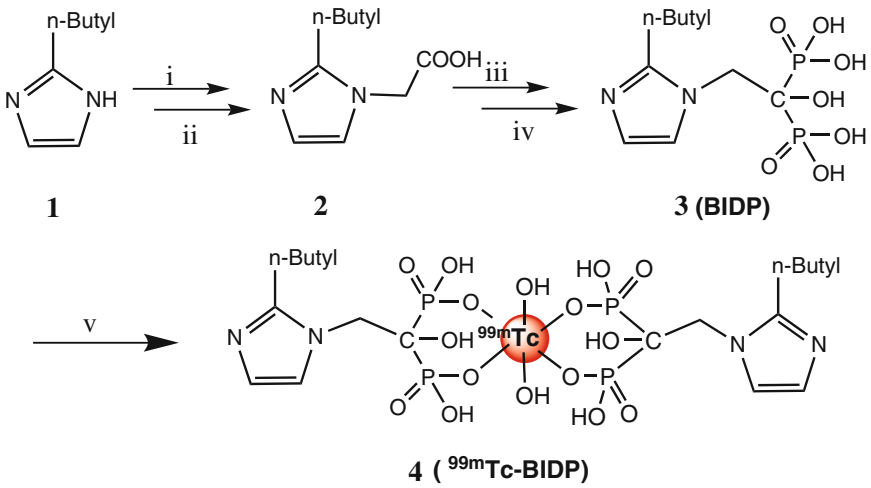

Scheme 2 Synthesis of BIDP and ^{99m}Tc-BIDP: *i* $BrCH_2COOEt$, KOH, K_2CO_3, tetrabutyl ammonium bromide (TBAB), CH_2Cl_2, reflux, 7 h; *ii* HCl, H2O, reflux, 7 h; *iii* PCl_3, H_3PO_4 (85 %), PhCl, 120 °C, 10 h; *iv* HCl, H_2O, reflux, 5 h; *v* $SnCl_2$, $Na^{99m}TcO_4$, PBS (pH 6.0), 100 °C, 20 min

200 μL of MS and HS, respectively. After incubation at 37 °C for 1–6 h, an aliquot of HS and MS solution were added to 100 μL of 50 % trifluoroacetic acid (TFA). After centrifugation, the upper solution was taken for TLC analysis.

Octanol–water partition coefficient

The octanol–water partition coefficient (log *P*) was determined for ^{99m}Tc-BIDP at pH 7.4 by measuring the radioactivity of the radiolabeled compound in octanol and PBS at equilibrium, respectively. First, ^{99m}Tc-BIDP solution was diluted with PBS (100 + 900 μL). Then, the solution was further mixed with 1.0 mL octanol, vortexed for 5 min, and centrifuged at 4,000 rpm for 5 min to ensure complete separation of layers. An aliquot (100 μL) of organic and aqueous phases were collected and the radioactivity was measured with a γ counter. The log *P* was calculated using the formula log P = log (radioactivity in octanol layer/radioactivity in PBS layer). The reported value is the average obtained from three independent experiments.

Plasma protein binding assay

^{99m}Tc-BIDP (100 μL, 37 KBq) was mixed with the human plasma (100 μL) in the centrifuge tube. After the mixture was incubated at 37 °C for 2 h, the plasma protein was precipitated by adding 1.0 mL trichloroacetic acid (TCA, 250 g L^{-1}) to the mixture. The supernatant and precipitate were separated by centrifugation at 4,000 rpm for 5 min. The radioactivities of both phases were measured separately. The above procedure was repeated thrice. The percentage of protein binding was determined by the following equation: Plasma binding % = [Precipitate $CPM/$(Precipitate CPM + Supernatant CPM)] $*$ 100 %

Pharmacokinetics

For pharmacokinetic analysis, six ICR mice were intravenously injected with 7.4 MBq of ^{99m}Tc-BIDP. Blood samples were drawn from each rat through the tail vein by microliter pipette (20 μL) at several time points between 5 min and 6 h after injection. The radioactivity of each blood sample was measured for by the γ counter and expressed as a percentage of the injected dose per gram of blood (% ID g^{-1}). Pharmacokinetic parameters were calculated using 3P97 software (edited by Chinese Mathematical Pharmacology, 1997, Beijing, China) (Xue *et al.*, 1997). In the present work, the pharmacokinetic of ^{99m}Tc-BIDP can be described by the following biexponential equation: $C = Ae^{-\alpha t} + Be^{-\beta t}$, where *A* and *B* are the extrapolated zero-time intercepts of the distribution and elimination phases, respectively; *C* is the plasma level of the tracer at any given time *t*; and α and β are rate constants of distribution and elimination phases, respectively.

Biodistribution studies

^{99m}Tc-BIDP (7.4 MBq, 0.2 mL) was administered to ICR mice via the tail vein injection. The mice were sacrificed by decapitation at 5, 10, 15, 30, 60, 120, and 240 min post injection. Interested organs were collected and weighed, and 200 μL of blood were taken from carotid artery. Their radioactivities were measured by a γ counter and expressed as % ID g^{-1} to determine the percentage of radioactivity absorbed by the organ or tissue. Then, the distribution in different organs was determined and the uptake rations of bone to other soft tissues were also obtained from the % ID g^{-1} values. The experiment at each time point was repeated five times. The data were expressed as mean values with standard deviations.

Bone imaging of rabbit

In order to comprehensively investigate the whole body localization of ^{99m}Tc-BIDP, SKY Light ECT was used to study the imaging of the rabbit. Prior to scanning, two New Zealand rabbits were anesthetized with ethyl carbamate solution (8.0 mL, 25 %) and fixed on the board. Pediatric urine bag was used to absorb the urine. Then ^{99m}Tc-BIDP (1.5 mL, 92.5 MBq) was injected intravenously into the rabbit through the marginal ear vein and bone scanning was carried out subsequently with ECT. The whole body image was observed and collected for 4 h. During the first hour, scanning images were collected every 5 min under the conditions of low energy, high resolution, and 128 × 128 matrix. Regions of interest (ROIs) were directly drawn on the SPECT composite image including bone, muscle, heart, liver, kidney, and stomach. Shapes and sizes of ROIs were kept constant for all subsequent images. The uptakes of femur, muscle close to femur, and other soft tissues were obtained, and the uptake ratios of bone to soft tissues were calculated from the same ROIs. Then, a series of static bone scanning images were collected at 1, 2, 3, and 4 h, respectively.

Results and discussion

Chemistry and radiolabeling

Compound **2** was prepared through the *N*-alkylation reaction and phase transfer catalytic (PTC) reaction, as illustrated in Scheme 3. To accelerate the reaction rate and achieve a satisfactory yield, TBAB was added to the reaction system as a phase transfer catalyst (Hui *et al.*, 1999). Then, BIDP was obtained through the phosphine acidification reaction of the carboxylic acid. Noteworthy is that the speed of adding PCl_3 has critical effect on the yield of the reaction. If the addition is fast, the reaction may be hard to control and the yield is also low. Otherwise, the reaction time may be too long. A moderate speed (about 0.4 mL min^{-1}) should be selected to control the reaction temperature and increase the yield. The structure of BIDP and intermediate were confirmed by melting point, mass spectra, IR, ^{1}H, and ^{13}C NMR spectra.

2-(2-Butyl-1H-imidazole-1-yl)acetic acid: yield: 26.6 %. mp: 138–141 °C; IR (KBr)/cm^{-1}: 3,395 (ν_{O-H}), 1,726 ($\nu_{C=O}$), 1,398 (ν_{C-N}); MS(ESI): $m/z = 182$ (found: 181); ^{1}H-NMR (400 MHz, DMSO): δ7.63 (d, 1H, CH-ring), 7.57 (d, 1H, CH-ring), 5.14 (s, 2H, COOH$\underline{CH_2}$), 2.90 (t, 2H, $CH_3CH_2CH_2\underline{CH_2}$), 1.61 (m, 2H, $CH_3CH_2\underline{CH_2}$), 1.25 (m, 2H, $CH_3\underline{CH_2}$), 0.85 (t, 3H, $CH_2\underline{CH_3}$); ^{13}C-NMR (100 MHz, D_2O): δ170.02 (s, COOH), 148.70 (s, N=C–N), 122.85 (s, C-ring), 118.02 (s, C-ring), 48.27 (s, N–$\underline{CH_2}$), 27.97 (s, $CH_3CH_2\underline{CH_2}$), 23.76 (s, ring-$\underline{CH_2}$), 21.38 (s, $\underline{CH_2}CH_3$), 12.78 (s, CH_3).

1-Hydroxy-2-(2-butyl-1H-imidazole-1-yl) ethylidene-1,1-diphosphonic acid (BIDP): yield: 17.1 %. mp: 54–56 °C; IR (KBr)/cm^{-1}: 3,410(ν_{O-H}), 7,55 (ν_{P-C}), 1,605 ($\nu_{C=N}$); MS(ESI): $m/z = 328$ (found: 329); ^{1}H-NMR (400 MHz, NaOH/D_2O): δ7.38 (d, 1H, CH-ring), 7.13 (d, 1H, CH-ring), 4.50 (s, 2H, NH$\underline{CH_2}$), 2.98 (t, 2H, $CH_3CH_2CH_2\underline{CH_2}$), 1.60 (m, 2H, $CH_3CH_2\underline{CH_2}$), 1.25 (m, 2H, $CH_3\underline{CH_2}$), 0.79 (t, 3H, $CH_2\underline{CH_3}$); ^{13}C-NMR (100 MHz, D_2O): δ151.56 (s, N=C–N), 123.94 (s, C-ring), 123.15 (s, C-ring), 75.57 (t, P–C–P), 50.29 (s, N–$\underline{CH_2}$), 29.40 (s, $CH_3CH_2\underline{CH_2}$), 25.88 (s, ring-$\underline{CH_2}$), 21.78 (s, $\underline{CH_2}CH_3$), 13.27 (s, CH_3).

BIDP was further radiolabeled by $Na^{99m}TcO_4$ with deoxidation of stannous chloride. Also noteworthy is that the pH value is very important for the radiolabeling of BIDP. When the acidity of the reaction system is high (pH 1–3), the RLY will be less than 90 % due to the fact that $^{99m}TcO_4^-$ is not completely reduced in a strong acidic condition. On the contrary, when the pH is larger than 6, $Na^{99m}TcO_4$ will be easily changed into the colloid of ^{99m}Tc by $SnCl_2$ under the alkaline condition, and therefore, the RLY will decrease significantly. So, the best pH is 4–6 where the RLY can be more than 95 %. The effect of other factors on the labeling yield, such as the amount of $SnCl_2 \bullet 2H_2O$, DP, and $^{99m}TcO_4^-$, has also been investigated according to the previous studies (Motaleb *et al.*, 2011; Qiu *et al.*, 2012). This labeling method also meets the clinical requirement for the production of other ^{99m}Tc-labeled diphosphonates, such as ^{99m}Tc-MDP.

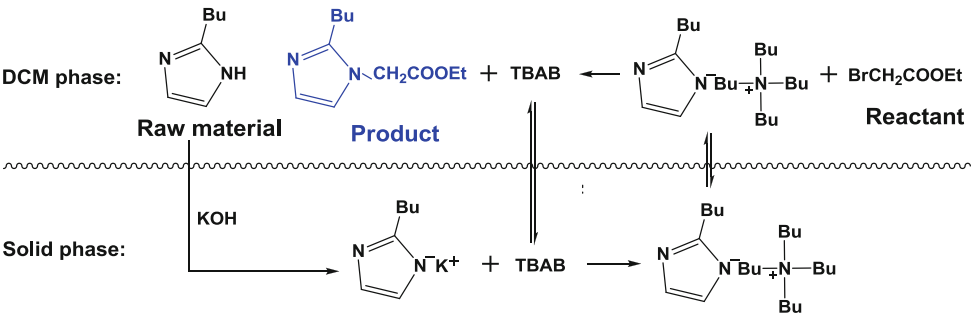

Scheme 3 Mechanism of phase transfer reaction

Quality control

The radio-TLC analysis was used to monitor the progress of the radiolabeling reaction and check the purity of the radiolabeled compound. All of the chemical species involved in the radiolabeling reaction were separated by TLC method (Fig. 1a). In the system of distilled water, $^{99m}TcO_2{\cdot}nH_2O$ remained at the origin (R_f = 0–0.1), while $Na^{99m}TcO_4$ and ^{99m}Tc-BIDP both migrate with the solvent front (R_f = 0.8–1.0). In the system of acetone, $^{99m}TcO_2{\cdot}nH_2O$ and ^{99m}Tc-BIDP remain at the origin (R_f = 0–0.1), while $Na^{99m}TcO_4$ migrated with the solvent front (R_f = 0.9–1.0). Under optimal radiolabeling condition, TLC analysis showed that $Na^{99m}TcO_4$ was completely reduced and ^{99m}Tc-colloidal amount was less than 2 %.

The HPLC analyses of ^{99m}Tc-BIDP and $Na^{99m}TcO_4$ were shown in Fig. 1b. It was observed that the retention time of ^{99m}Tc-BIDP was 2.8 min, while that of $Na^{99m}TcO_4$ was 8.9 min. The single peak suggested that only one product (^{99m}Tc-BIDP) was formed. The specific activity of the radiotracer at the end of synthesis was estimated to be about 32 GBq/mmol. This value is comparable to that of other technetium-99 m labeled small molecule drug (Nayak *et al.*, 2008). Since the radiotracer was used immediately after preparation for both in vitro and in vivo studies, the RCP was identical to the RLY. Therefore, the RCP of ^{99m}Tc-BIDP was also larger than 95 %.

In vitro stability

The stability was assessed by measuring the RCP based on the TLC analysis. As shown in Fig. 2, more than 95 % of ^{99m}Tc-BIDP remained intact in the MS and HS after 6 h of incubation. This suggested that the radiolabeling efficiency was high and ^{99m}Tc-BIDP was stable enough to allow further biological and imaging studies.

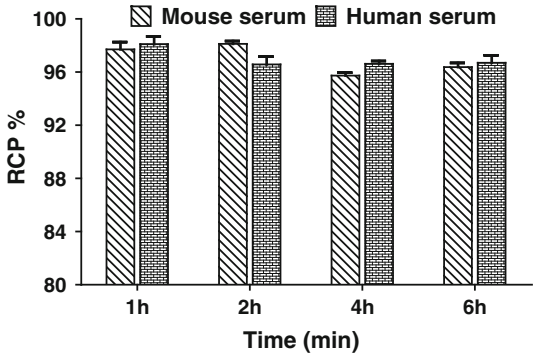

Fig. 2 RCP of ^{99m}Tc-BIBDP in mouse serum and human serum determined by TLC analysis after incubation for 1, 2, 4, and 6 h, respectively

Log *P* and plasma protein binding

The octanol–water partition coefficient (log *P*) of ^{99m}Tc-BIDP was determined to be −1.55, indicating that ^{99m}Tc-BIDP has high hydrophilic property. This may be attributed to the fact that the structure contains many hydroxyl groups and an imidazole ring. Compared with previous studies, we have found that the lipophilicity of ^{99m}Tc-BIDP was higher than ^{99m}Tc-MIDP, ^{99m}Tc-EIDP, and ^{99m}Tc-PIDP (Luo *et al.*, 2005; Niu *et al.*, 2008; Chen *et al.*, 2009). Since log *P* is an important parameter for assessing the biological distribution of these complexes (Valko, 2004), higher lipid molecules have more positive effect on the bone binding model (Zhang *et al.*, 2009). Thus, it is speculated that ^{99m}Tc-BIDP has more positive effect on the bone uptake than the previous ^{99m}Tc-DPs.

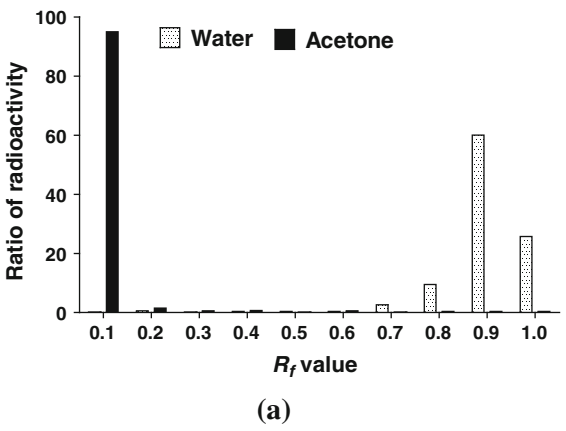

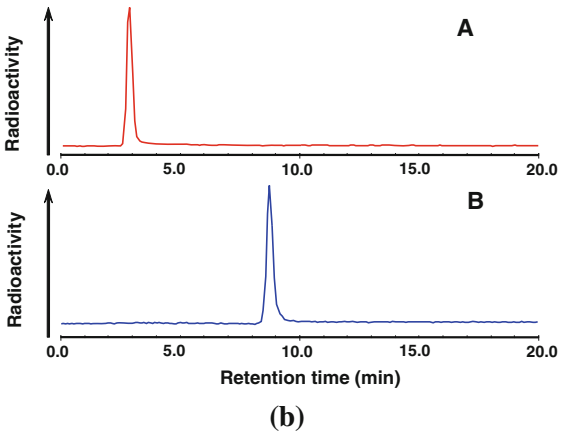

Fig. 1 **a** RCP of ^{99m}Tc-BIDP in the acetone and water estimated by TLC. **b** RP-HPLC radioanalysis of ^{99m}Tc-BIDP (*A*) and $Na^{99m}TcO_4$ (*B*). Conditions: C18 reversed-phase column (10 μm, 250 × 4.6 mm), flow rate of 1.0 mL min^{-1} with CH_3CN (30 %) and H_2O (70 %). ^{99m}Tc-BIDP: Rt = 2.8 min, $Na^{99m}TcO_4$: Rt = 8.9 min

The percentage of protein binding was 58.93 % for ^{99m}Tc-BIDP. In general, the plasma protein binding efficiency also has significant influence on the bone uptake (Kroesbergen *et al.*, 1988). Compared with ^{99m}Tc-MIDP, ^{99m}Tc-EIDP, and ^{99m}Tc-PIDP (Luo *et al.*, 2005; Niu *et al.*, 2008; Chen *et al.*, 2009), ^{99m}Tc-BIDP has higher plasma protein binding. It turned out that with the extension alkyl chain in the ring, the plasma protein binding increases and the blood clearance will decrease. The blood clearance will be discussed in detail in the pharmacokinetic studies.

Pharmacokinetics of ^{99m}Tc-BIDP

In Fig. 3, a correlation between the blood radioactivity and time has been plotted for ^{99m}Tc-BIDP, which shows that the complex can be washed out quickly from the blood. And the blood clearance of ^{99m}Tc-BIDP accords well with a double exponential equation, $C = 5.891e^{-0.0224t} + 14.27e^{-0.420t} + 0.3063$. The distribution half-life ($t_{1/2\alpha}$) and elimination half-life ($t_{1/2\beta}$) of ^{99m}Tc-BIDP were 1.65 and 30.91 min, respectively. This indicates that ^{99m}Tc-BIDP can be quickly absorbed by the blood and also eliminated rapidly from the blood (Liu *et al.*, 2009).

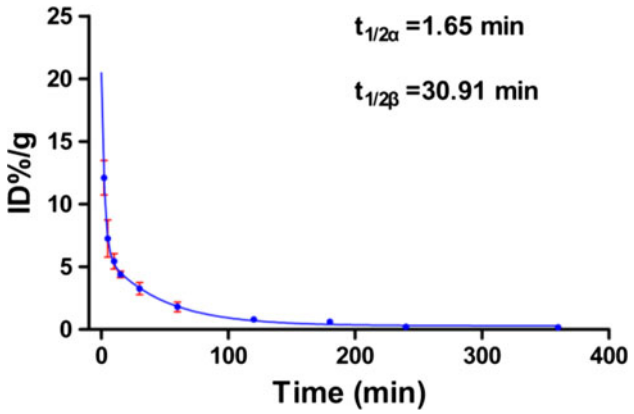

Fig. 3 Pharmacokinetic curve of ^{99m}Tc-BIDP in mice ($n = 5$, mean ± SD). $t_{1/2\alpha}$: distribution half-life, $t_{1/2\beta}$: elimination half-life

Biodistribution

Although ZL has been known to possess low toxicity and been used therapeutically at a high dose (Berenson *et al.*, 2005), the toxicity profile of its derivatives is uncertain. In the period of biodistribution study, the mice were watched carefully for any sign of adverse reaction after the radiotracer ^{99m}Tc-BIDP was given via intravenous injection, respectively. Through the study period of 4 h, the mice showed no sign of toxicity. The biodistribution data of ^{99m}Tc-BIDP in normal mice have been listed in Table 1. It was observed that ^{99m}Tc-BIDP can reach the skeleton within 5 min after injecting, especially quickly for the joint. The amount of ^{99m}Tc-BIDP deposited in the bone began to increase continuously to a maximum of 24.60 %ID g^{-1} at 120 min. It has been proved that ^{99m}Tc-MIDP, ^{99m}Tc-EIDP, and ^{99m}Tc-PIDP have excellent bone binding efficiency. In order to better evaluate the bone uptake efficiency, the bone uptake of ^{99m}Tc-BIDP will be compared with them, as shown in Fig. 4. It was observed that the bone uptake of ^{99m}Tc-BIDP was higher than ^{99m}Tc-MIDP, ^{99m}Tc-EIDP, and ^{99m}Tc-PIDP at 15 min and 120 min. The results clearly show that an increase in the lipophilicity of the DP ligand through extending the alkyl chain in the imidazolyl group leads to the tendency of targeting and accumulation of ^{99m}Tc-DPs to the bone. It was also noteworthy that compared with those of the

Table 1 Biodistribution of ^{99m}Tc-BIDP in normal mice (mean ± SD, $n = 5$)

Organ	5 min	10 min	15 min	30 min	60 min	120 min	240 min
$a_{m,\ Heart}$	4.30 ± 0.85	3.60 ± 0.22	3.08 ± 0.14	1.61 ± 0.17	0.96 ± 0.12	0.50 ± 0.02	0.49 ± 0.09
$a_{m,\ Liver}$	4.95 ± 0.44	6.13 ± 0.75	7.81 ± 0.35	3.73 ± 0.69	2.89 ± 0.22	2.65 ± 0.27	2.52 ± 0.49
$a_{m,\ Spleen}$	2.63 ± 0.38	2.09 ± 0.04	2.11 ± 0.20	1.28 ± 0.06	0.80 ± 0.09	0.61 ± 0.05	0.59 ± 0.07
$a_{m,\ Lung}$	10.8 ± 0.22	8.14 ± 0.32	6.73 ± 0.45	3.84 ± 0.30	2.21 ± 0.15	1.29 ± 0.08	0.96 ± 0.24
$a_{m,\ Kidneys}$	12.7 ± 0.31	15.4 ± 1.29	13.8 ± 1.86	8.61 ± 1.11	7.07 ± 0.73	6.27 ± 0.45	5.95 ± 0.60
$a_{m,\ Bone\ +\ Joint}$	9.61 ± 0.78	12.1 ± 0.20	14.6 ± 0.89	15.2 ± 1.16	22.8 ± 2.32	24.6 ± 1.65	18.9 ± 1.44
$a_{m,\ Joint}$	12.38 ± 1.61	17.4 ± 1.55	18.3 ± 2.55	19.6 ± 1.96	24.5 ± 1.10	27.3 ± 6.37	21.3 ± 4.29
$a_{m,\ Muscle}$	2.33 ± 0.20	2.01 ± 0.21	2.31 ± 0.18	0.95 ± 0.06	0.61 ± 0.11	0.25 ± 0.03	0.17 ± 0.15
$a_{m,\ Gonad}$	1.39 ± 0.17	1.67 ± 0.20	1.88 ± 0.25	0.96 ± 0.05	0.66 ± 0.09	0.31 ± 0.04	0.34 ± 0.02
$a_{m,\ Intestines}$	2.73 ± 0.32	3.78 ± 0.18	3.60 ± 0.40	1.80 ± 0.32	1.20 ± 0.22	0.86 ± 0.09	1.07 ± 0.19
$a_{m,\ Stomach}$	3.12 ± 0.31	7.94 ± 0.63	9.65 ± 1.23	7.03 ± 0.79	6.50 ± 1.85	4.84 ± 1.10	6.62 ± 0.72
$a_{m,\ Brain}$	0.38 ± 0.09	0.30 ± 0.03	0.34 ± 0.02	0.18 ± 0.01	0.11 ± 0.01	0.04 ± 0.00	0.09 ± 0.01

a_m denotes the percentage uptake of the injected dose per gram of tissues (% ID g^{-1}), where 'a' means the radioactivity uptake and 'm' means the weight

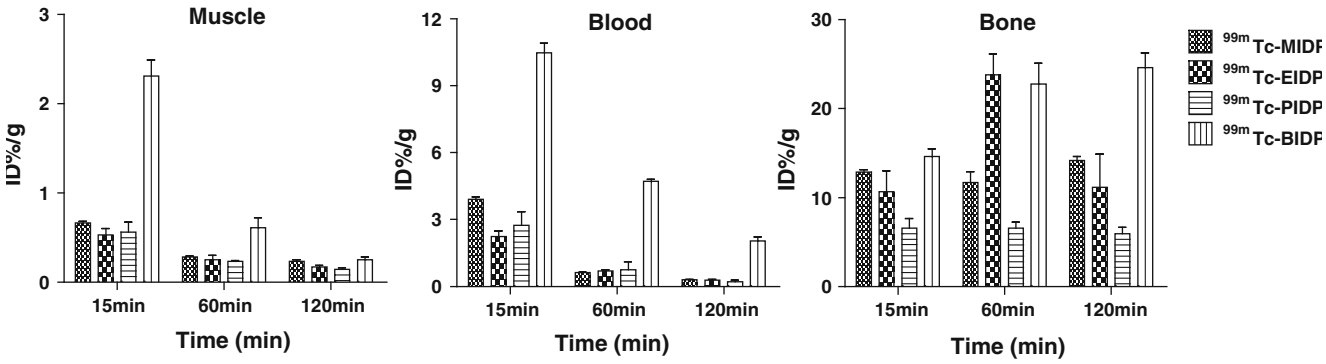

Fig. 4 Comparison of ^{99m}Tc-MIDP, ^{99m}Tc-EIDP, ^{99m}Tc-PIDP, and ^{99m}Tc-BIDP in mice

clinically widely used bone imaging agent ^{99m}Tc-MDP, the bone uptake of ^{99m}Tc-BIDP were all higher than those of ^{99m}Tc-MDP (Liu *et al.*, 2004).

Moreover, the uptake of ^{99m}Tc-BIDP in blood and muscle were also higher than those of ^{99m}Tc-MIDP, ^{99m}Tc-EIDP, and ^{99m}Tc-PIDP, which can be observed intuitively from Fig. 4. This may be attributed to the fact that ^{99m}Tc-BIDP has a higher Log *P* value and plasma protein binding. However, at 60–120 min post injection, the uptakes in the blood and the muscle among these ^{99m}Tc-DPs are similar. In addition, the bone uptake of ^{99m}Tc-BIDP increased to a maximum of 24.60 % ID g^{-1} at 120 min. These results indicate that ^{99m}Tc-BIDP has larger uptake ratios of bone to blood and muscle among ^{99m}Tc-MIDP, ^{99m}Tc-EIDP, ^{99m}Tc-PIDP, and ^{99m}Tc-BIDP. Among all the non-target organs, the kidney uptake of ^{99m}Tc-BIDP was the highest but the concentration decreased quickly. It decreased from 12.7 % ID g^{-1} at 5 min to 7.07 % ID g^{-1} at 60 min. Therefore, a conclusion was drawn that ^{99m}Tc-BIDP can be excreted rapidly through urine. As a whole, the radiotracer ^{99m}Tc-BIDP has higher bone uptake and lower background at 60 min post injection, compared to ^{99m}Tc-MIDP, ^{99m}Tc-EIDP, and ^{99m}Tc-PIDP. In comparison with its analogs of ^{99m}Tc-labeled disubstituted zoledronic acids [^{99m}Tc-DMIDP (Qiu *et al.*, 2012) and ^{99m}Tc-EMIDP (Lin *et al.*, 2010)], the radiotracer ^{99m}Tc-BIDP also displays significantly higher bone to muscle uptake ratios from 60 min post injection. For instance, at 60 min the bone to muscle uptake ratio of ^{99m}Tc-BIDP (37.37) was larger than those of ^{99m}Tc-DMIDP (30.67) and ^{99m}Tc-EMIDP (29.79). At 120 min post injection, the bone to muscle uptake ratio of ^{99m}Tc-BIDP was much larger than those of ^{99m}Tc-DMIDP and ^{99m}Tc-EMIDP (98.40 vs. 60.25 and 33.04). The higher target-to-background ratio will help to obtain a clearer skeletal image. This indicates that ^{99m}Tc-BIDP is excellent

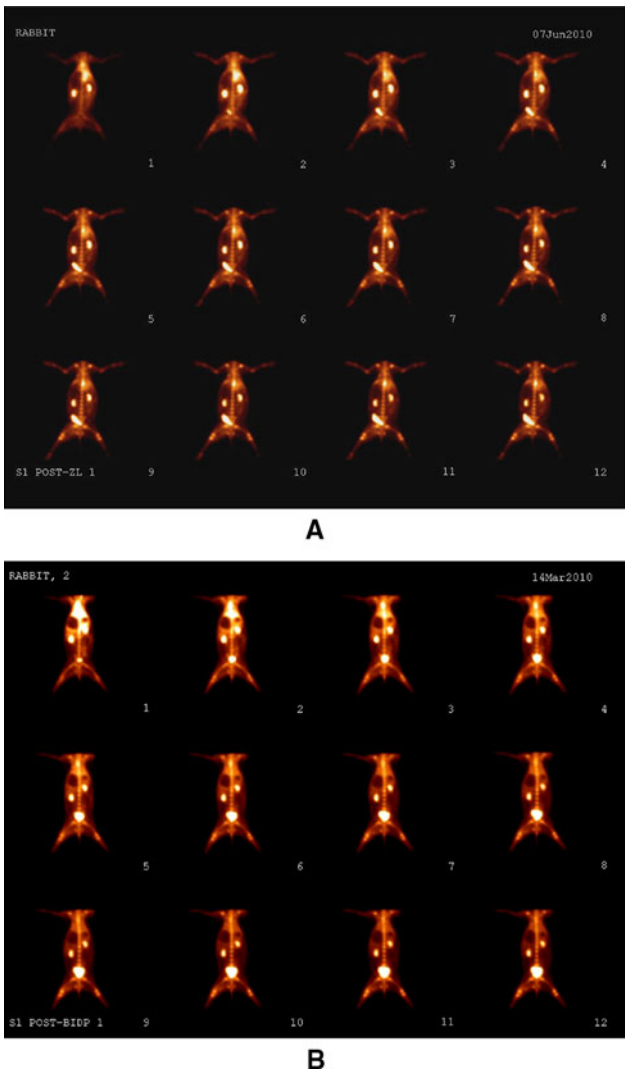

Fig. 5 Dynamic images of rabbit bone scanning in 1 h post injection of ^{99m}Tc-ZL (**a**) and ^{99m}Tc-BIDP (**b**)

and it holds great potential as a promising diagnostic radiopharmaceutical.

Bone imaging

Dynamic images

In order to better evaluate the bone imaging efficiency and biodistribution as well as clearance of ^{99m}Tc-BIDP in vivo, bone scanning images of the normal rabbit after intravenous administration of ^{99m}Tc-BIDP were collected dynamically and compared with those of ^{99m}Tc-ZL, which have been presented in Fig. 5. It was observed that these two compounds exhibited similar behavior in vivo, which mainly accumulated in the skeleton, kidney, and urinary bladder. It also demonstrated that ^{99m}Tc-BIDP was metabolized through the kidney of the rabbit, which is consistent with the biodistribution result of the mouse. Also noteworthy is that a clear image of the rabbit skeleton can be obtained at 1 h after injecting ^{99m}Tc-BIDP. This reveals that ^{99m}Tc-BIDP has highly selective bone uptake and rapid clearance from soft tissues in the rabbit after the first hour, which accords well with the biodistribution studies in mice.

Static images

For comparison, a series of static images of the rabbit bone scanning after intravenous administration of ^{99m}Tc-BIDP and ^{99m}Tc-ZL, respectively, were also collected in Fig. 6. From these images, one can see that two radiolabeled complexes are all excreted from the kidney, and ^{99m}Tc-BIDP has highly selective skeletal uptake in the rabbit at different time intervals after intravenous injection. However, it is notable that ^{99m}Tc-BIDP is eliminated faster from the liver than ^{99m}Tc-ZL, and more satisfactory images can be obtained from ^{99m}Tc-BIDP. The rabbit SPECT imaging results agree well with the biodistribution studies in mice and suggest that ^{99m}Tc-BIDP possesses excellent characteristics for the potential application as a bone scanning agent. However, utilizing a bone pathology model to compare the bone lesion with the normal bone uptake will be necessary to more fully assess the clinical utility of ^{99m}Tc-BIDP. This will be taken into account in the subsequent research.

Conclusion

In summary, a novel radiotracer ^{99m}Tc-BIDP was prepared with high radiolabeling yield, radiochemical purity, and stability. Kinetics of blood clearance showed that ^{99m}Tc-BIDP can be quickly absorbed by the blood and also eliminated from the blood rapidly. In the biodistribution studies, from ^{99m}Tc-MIDP to ^{99m}Tc-BIDP with the lipid solubility increasing, ^{99m}Tc-BIDP exhibits significant advantages on the bone uptake. At 1 h post injection, excellent images of the rabbit skeleton can be obtained from^{99m}Tc-BIDP, which was faster than ^{99m}Tc-ZL. So, ^{99m}Tc-BIDP displays attractive features as a promising

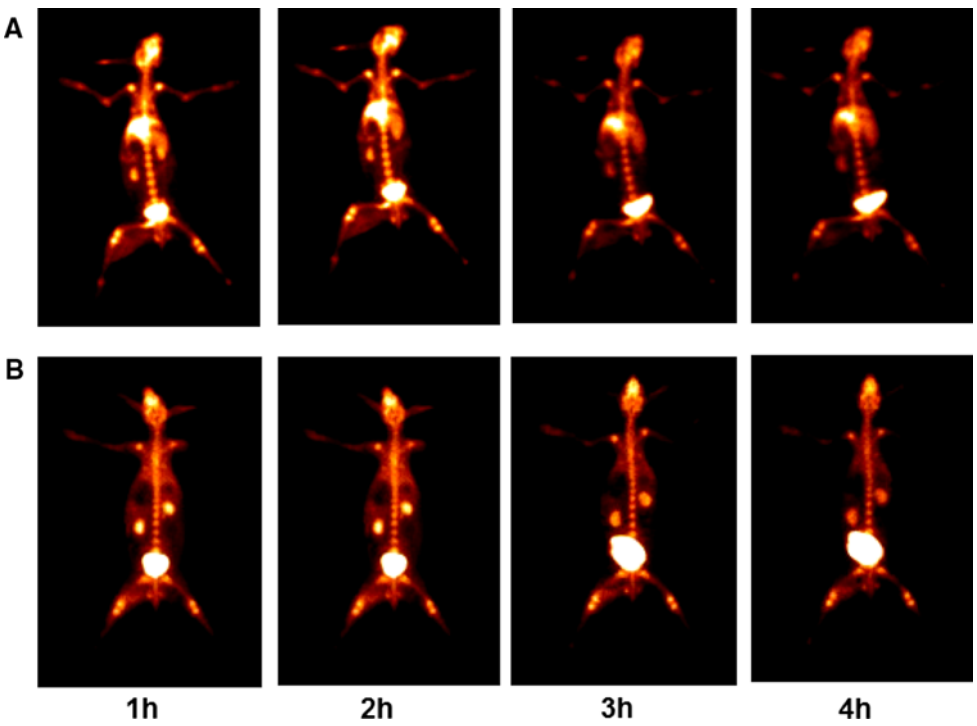

Fig. 6 Static images of the rabbit bone scanning from 1 to 4 h post injection of ^{99m}Tc-ZL (**a**) and ^{99m}Tc-BIDP (**b**)

bone scanning agent, and it is worth of further investigation as a novel SPECT imaging agent in larger animals or animals with bone metastases.

Acknowledgments This work was financially supported by the National Natural Science Foundation of China (20801024 and 21001055), Key Medical Talent Project of Jiangsu Province (RC2011097) and Public Service Platform for Science and Technology Infrastructure Construction Project of Jiangsu Province (BM2012066). The authors also wish to thank Dr Wanzhong Ye for his assistance in the SPECT scanning.

References

Berenson JR (2005) Recommendations for zoledronic acid treatment of patients with bone metastases. Oncologist 10:52–62

Bevan JA, Tofe AJ, Benedict JJ, Francis MD, Barnett BL (1980) Tc-99m HMDP (hydroxymethylene diphosphonate): a radiopharmaceutical for skeletal and acute myocardial infarct imaging. II. Comparison of Tc-99m hydroxymethylene diphosphonate (HMDP) with other technetium-labeled bone-imaging agents in a canine model. J Nucl Med 21(10):967–970

Chen CQ, Luo SN, Lin JG, Yang M, Ye WZ, Qiu L (2009) Preparation and biodistribution of ^{99m}Tc-PIDP as bone imaging agent. Nucl Sci Tech 20:302–306

Hui XP, Zhang LM, Zhang ZY (1999) Application of phase transfer catalysis in heterocyclic chemistry. Chinese J Org Chem 19: 458–467

Jurisson SS, Lydon JD (1999) Potential technetium small molecule radiopharmaceuticals. Chem Rev 99(9):2205–2218

Kroesbergen J, Roozen AMP, Wortelboer MR, Gelsema WJ, DeLigny CL (1988) ^{99m}Tc bone scanning agents-VI. Gel chroma-tographic analysis of the plasma protein binding of ^{99m}Tc(Sn)pyrophosphate, ^{99m}Tc(Sn)MDP and ^{99m}Tc(Sn)HMDP. Nucl Med Biol 15(5):479–487

Lin JG, Luo SN, Chen CQ, Qiu L, Wang Y, Cheng W, Ye WZ, Xia YM (2010) Preparation and preclinical pharmacological study on a novel bone imaging agent ^{99m}Tc-EMIDP. Appl Radiat Isot 68(9):1616–1622

Lin JG, Qiu L, Cheng W, Luo SN, Ye WZ (2011) Preparation and in vivo biological investigations on a novel radioligand for bone scanning: technetium-99m-labeled zoledronic acid derivative. Nucl Med Biol 38:619–629

Liu LQ, Li ZM, Wang XB (2004) The systhesis and study of a new kind of bone imaging agent ^{99m}Tc-EDP. J Beijing Norm Univ 40(1):75–79

Liu RS, Chou TK, Chang CH, Wu CY, Chang CW, Chang TJ, Wang SJ, Lin WJ, Wang HE (2009) Biodistribution, pharmacokinetics and PET Imaging of [^{18}F]FMISO, [^{18}F]FDG and [^{18}F]FAc in a sarcoma and inflammation bearing mouse model. Nucl Med Biol 36(3):305–312

Love C, Din AS, Tomas MB, Kalapparambath TP, Palestro CJ (2003) Radionuclide bone imaging: an illustrative review. Radiographics 23:341–358

Luo SN, Wang HY, Xie MH (2005) The study on the preparation and biodistribution of ^{99m}Tc-MIDP. Chin J Nucl Med 6:342–343

Motaleb MA, Sakr TM (2011) Synthesis and preclinical pharmacological evaluation of ^{99m}Tc-TEDP as a novel bone imaging agent. J Label Compd Radiopharm 54(9):597–601

Nayak TK, Hathaway HJ, Ramesh C, Arterburn JB, Dai DH, Sklar LA, Norenberg JP, Prossnitz ER (2008) Preclinical development of a neutral, estrogen receptor targeted, tridentate ^{99m}Tc(I)-estradiol-pyridin-2-yl hydrazine derivative for imaging of breast and endometrial cancers. J Nucl Med 49(6):978–986

Niu GS, Luo SN, Yan XH, Yang M, Ye WZ, Wang HY (2008) The preparation and biodistribution of ^{99m}Tc-EIDP. Nucl Tech (in Chinese) 31:698–701

Ogawa K, Mukai T, Inoue Y, Ono M, Saji H (2006) Development of a novel ^{99m}Tc-chelate conjugated bisphosphonate with high affinity for bone as a bone scintigraphic agent. J Nucl Med 47(12): 2042–2047

Pauwels EK, Stokkel MP (2001) Radiopharmaceuticals for bone lesions. Imaging and therapy in clinical practice. Q J Nucl Med 45(1):18–26

Qiu L, Lin JG, Luo SN, Wang Y, Cheng W, Zhang S (2012) A novel ^{99m}Tc-labeled dimethyl-substituted zoledronic acid (DMIDP) with improved bone imaging efficiency. Radiochim Acta 100: 463–471

Robert EC, Eugene VM (2011) Bisphosphonates in oncology. Bone 49:71–76

Smith MR (2008) Osteoclast targeted therapy for prostate cancer: bisphosphonates and beyond. Urol Oncol Semin Ori 26(4):420–425

Subramanian G, McAfee JG, Blair RJ, Mehter A, Connor T (1972) ^{99m}Tc-EHDP: a potential radiopharmaceutical for skeletal imaging. J Nucl Med 13(12):947–950

Subramanian G, McAfee JG, Blair RJ, Kallfelz KF, Thomas FD (1975) Technetium-99m-methylene diphosphonate: a superior agent for skeletal imaging: comparison with other technetium complexes. J Nucl Med 16(8):744–755

Valko K (2004) Application of high-performance liquid chromatography based measurements of lipophilicity to model biological distribution. J Chromatogr A 1037:299–310

Vasireddy S, Talwarkar A, Miller H (2003) Patterns of pain in Paget's disease of bone and their outcomes on treatment with pamidronate. Clin Rheumatol 22(6):376–380

Widler L, Jaeggi KA, Glatt M, Müller K, Bachmann R, Bisping M, Born AR, Cortesi R, Guiglia G, Jeker H, Klein R, Ramseier U, Schmid J, Schreiber G, Seltenmeyer Y, Green JR (2002) Highly potent geminal bisphosphonates. From pamidronate disodium (Aredia) to zoledronic Acid (Zometa). J Med Chem 45(17): 3721–3738

Xue FS, Liao X, Tong SY, Liu JH, Li L, Zou Q, Luo LK (1997) Pharmacokinetics of vecuronium during acute isovolaemic haemodilution. Brit J Anaesth 79(5):612–616

Zhang YH, Cao R, Yin FL, Hudock MP, Guo RT, Krysiak K, Mukherjee S, Gao YG, Robinson H, Song YC, No JH, Bergan K, Leon A, Cass L, Goddard A, Chang TK, Lin FY, Beek EV, Papapoulos S, Wang AHJ, Kubo T, Ochi M, Mukkamala D, Oldfield E (2009) Lipophilic bisphosphonates as Dual Farnesyl/Geranylgeranyl diphosphate synthase inhibitors: an X-ray and NMR investigation. J Am Chem Soc 131(14):5153–5162